

KCNE4 suppresses Kv1.3 currents by modulating trafficking, surface expression and channel gating

Laura Solé¹, Meritxell Roura-Ferrer^{*,1}, Mireia Pérez-Verdaguer¹, Anna Oliveras¹, Maria Calvo², José Manuel Fernández-Fernández³ and Antonio Felipe^{1,‡}

¹Molecular Physiology Laboratory, Departament de Bioquímica i Biologia Molecular, Institut de Biomedicina (IBUB), Universitat de Barcelona, Avda. Diagonal 645, 08028 Barcelona, Spain

²Departament de Biologia Cel·lular, Institut d'Investigacions Biomèdiques August Pi i Sunyer, Universitat de Barcelona, 08036 Barcelona, Spain

³Laboratory of Molecular Physiology and Channelopathies, Departament de Ciències Experimentals i de la Salut, Universitat Pompeu Fabra, Dr Aiguader 88, 08003, Barcelona, Spain

*Present address: Unidad de Biofísica, CSIC-UPV/EHU, Universidad del País Vasco, Barrio Sarriena s/n, 48940 Leioa, Spain

‡Author for correspondence (afelipe@ub.edu)

Accepted 9 August 2009

Journal of Cell Science 122, 3738-3748 Published by The Company of Biologists 2009

doi:10.1242/jcs.056689

Summary

Voltage-dependent potassium channels (Kv) play a crucial role in the activation and proliferation of leukocytes. Kv channels are either homo- or hetero-oligomers. This composition modulates their surface expression and serves as a mechanism for regulating channel activity. Kv channel interaction with accessory subunits provides mechanisms for channels to respond to stimuli beyond changes in membrane potential. Here, we demonstrate that KCNE4 (potassium voltage-gated channel subfamily E member 4), but not KCNE2, functions as an inhibitory Kv1.3 partner in leukocytes. Kv1.3 trafficking, targeting and activity are altered by the presence of KCNE4. KCNE4 decreases current density, slows activation, accelerates inactivation, increases cumulative inactivation, retains Kv1.3 in the ER and impairs channel targeting to lipid raft microdomains. KCNE4 associates with Kv1.3 in the ER and

decreases the number of Kv1.3 channels at the cell surface, which diminishes cell excitability. Kv1.3 and KCNE4 are differentially regulated upon activation or immunosuppression in macrophages. Thus, lipopolysaccharide-induced activation increases Kv1.3 and KCNE4 mRNA, whereas dexamethasone triggers a decrease in Kv1.3 with no changes in KCNE4. The channelosome composition determines the activity and affects surface expression and membrane localization. Therefore, KCNE4 association might play a crucial role in controlling immunological responses. Our results indicate that KCNE ancillary subunits could be new targets for immunomodulation.

Key words: KCNE regulatory subunits, Kv1.3, Leukocytes, Trafficking, Channelosome, Surface expression

Introduction

Voltage-dependent potassium channels (Kvs) play a crucial role in excitable cells by determining resting membrane potential and controlling action potentials (Hille, 2001). In addition, they are also involved in the immune system response. The activation and proliferation of leukocytes occurs via regulation of transmembrane ion fluxes, and increasing evidence indicates that some signaling occurs through K⁺ channels. Thus, changes in the membrane potential are among the earliest events that occur upon stimulation of leukocytes, and K⁺ channels underlie the Ca²⁺ signal involved in activation (Lewis and Cahalan, 1995; Cahalan et al., 2001; Panyi et al., 2004a).

The Kv1.3 channel (also known as KCNA3) is involved in the maintenance of the resting membrane potential in cells involved in the immune system, and several studies point to this protein as an excellent target for immunomodulation (Chandy et al., 2004; Beeton et al., 2005). Altered Kv1.3 expression is associated with autoimmune diseases such as multiple sclerosis, rheumatoid arthritis, psoriasis and type I diabetes, and Kv1.3-based therapies are effective in experimental models (Chandy et al., 2004; Beeton and Chandy, 2005; Beeton et al., 2006; Wulff and Pennington, 2007). In leukocytes, which express a restricted voltage-dependent K⁺ current phenotype, Kv1.3 is considered the major channel. However, we previously demonstrated that Kv1.3-Kv1.5 heteromeric channels contribute to the major K⁺ current in the myeloid lineage (Vicente

et al., 2006; Villalonga et al., 2007). In this scenario, the oligomeric structure of the Kv1.3 channelosome when associated with other partners could be involved a wide variety of physiological activities and immunological functions. Assigning specific K⁺ channel clones to native currents is often difficult as this complexity is enhanced by the presence of ancillary subunits. The interaction of Kv channels with Kv β modulatory subunits provides a mechanism for channels to respond to a variety of stimuli beyond changes in membrane potential (Martens et al., 1999; Li et al., 2006).

In addition to Kv β regulatory subunits, KCNE peptides, which have been widely studied in association with Kv7.1 and Kv11.1 cardiac channels, contribute to the functional diversity of K⁺ currents (McCrossan and Abbott, 2004). These interactions have been shown to be important in genetic disorders such as long QT syndrome, which are linked to KCNE mutations (Abbott and Goldstein, 2001; Abbott and Goldstein, 2002). The *KCNE* gene family comprises five known members, *KCNE1* to *KCNE5*. KCNE peptides can assemble promiscuously, yielding a wide variety of biophysically distinct channels (McCrossan and Abbott, 2004). Thus, cardiac Kv1.5 coimmunoprecipitates with KCNE1 and KCNE2 and the absence of *kcnk2* gene modifies the slow component of the delayed rectifying K⁺ current ($I_{K,slow}$) in the heart (Melman et al., 2004; Roepke et al., 2008). In addition, KCNE3 alters the gating of Kv3.4 and reduces Kv2.1 and Kv3.1 currents in the brain and skeletal muscle (Abbott et al., 2001; McCrossan et al., 2003;

Lewis et al., 2004). Finally, KCNE4 inhibits Kv1.1 and Kv1.3 currents (Grunnet et al., 2003). However, there is no evidence of their physical association, and contradictory results (Deschenes and Tomaselli, 2002; McCrossan et al., 2009) have raised doubts about the specificity of these modulatory actions without further analysis.

Several lines of evidence indicate that post-translational events are involved in leukocyte Kv1.3 regulation. Recently, there has been much interest in channel targeting to the membrane that defines the protein microenvironment. Membrane microdomains (lipid rafts) rich in cholesterol and sphingolipids function as platforms on which signal transduction pathways interface. Multiple Kv channels have affinities for lipid rafts and different isoforms are targeted to distinct lipid microdomains (Martens et al., 2004; Maguy et al., 2006). In this context, Kv1.3 is targeted to raft domains involved in immunological synapses in T-cells (Panyi et al., 2004b), but the association of Kv1.3 and Kv1.5 in macrophages alters trafficking and targeting. However, pro-inflammatory activation targets Kv1.3 back to lipid rafts (Martinez-Marmol et al., 2008; Vicente et al., 2008). These determinants affect the expression and functional properties of the channels and contribute to the diversity of K⁺ channels in leukocytes. Because KCNE peptides control gating and the surface expression of channels, we aimed to investigate whether KCNE4 associates with Kv1.3 to control channel expression. KCNE4, but not KCNE2, acts as a dominant negative Kv1.3 partner. Kv1.3 trafficking, targeting and activity are dramatically altered by the presence of KCNE4. Our results demonstrate, for the first time, that members of the Kv1 family (*Shaker*) associate with KCNE peptides, altering their surface expression and trafficking. Different K⁺ channel subunit compositions could lead to specific alteration in cellular excitability, thus determining specific cell responses. Therefore, the identification of the components of the channelosome and their regulation are essential for their possible use as therapeutic targets. The present report points to KCNE ancillary subunits as new targets in immunomodulation.

Results

KCNE4 modifies Kv1.3 gating and trafficking

HEK293 cells transfected with Kv1.3-YFP exhibited outward K⁺ currents at depolarizing potentials (Fig. 1A). The presence of KCNE4-CFP inhibited the peak current density. In addition, macroscopic currents suggested that KCNE4, but not KCNE2, modified the activation and inactivation kinetics. Unlike KCNE2, KCNE4 decreased the current density at all depolarized voltages by more than 50% (Fig. 1B). However, the threshold for activation was similar (−30 mV). Fig. 1C shows that KCNE4 slowed the activation time constant (τ) in all depolarized pulses. No currents were observed when depolarized pulses were applied to KCNE4- and KCNE2-transfected HEK293 cells (not shown).

Kv1.3 exhibits defined characteristics such as cumulative inactivation and C-type inactivation (Grissmer et al., 1990; Grissmer et al., 1994). KCNE4 increased the percentage and rate of cumulative inactivation of Kv1.3 (Fig. 1D). Kv1.3 exhibited 40% cumulative inactivation, but this value increased to 75% in the presence of KCNE4. In addition, cumulative inactivation, in the presence of KCNE4, occurred quickly and reached a plateau within the first 3 seconds (Fig. 1E). As expected from Fig. 1A, C-type inactivation was accelerated by KCNE4 (Fig. 1F). The effects of KCNE4 were specific because no changes were observed in the presence of KCNE2 (not shown).

Although KCNE4 inhibited Kv1.3 currents, changes in gating are not indicative of physiological interactions (Deschenes and

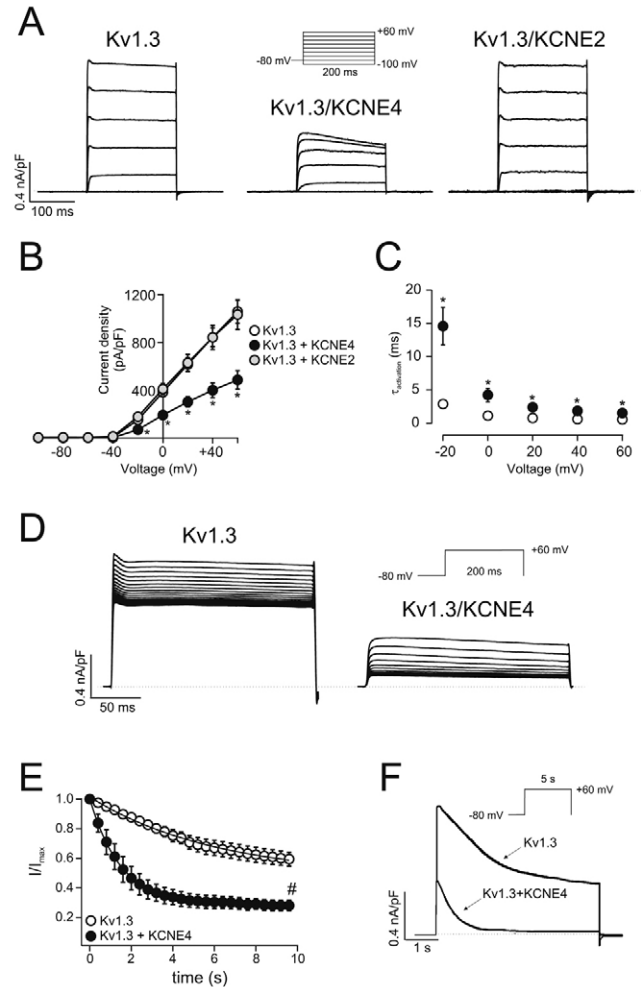


Fig. 1. KCNE4 modifies the gating of Kv1.3. (A) Representative current traces obtained from HEK293 cells expressing Kv1.3 alone (left), Kv1.3-KCNE4 (center) and Kv1.3-KCNE2 (right). (B) Current density (pA/pF) plotted against voltage (mV). Cells were clamped at −80 mV and current traces were elicited by 200 millisecond voltage steps to potentials ranging from −100 mV to +60 mV in 20-mV increments. White circles, Kv1.3 ($n=13$); black circles, Kv1.3-KCNE4 channels ($n=8$); gray circles, Kv1.3-KCNE2 ($n=6$). $*P<0.01$ (vs Kv1.3). (C) Time constant for activation ($\tau_{\text{activation}}$) at the indicated voltages, illustrating that activation time constants were slower for Kv1.3-KCNE4 channels. $*P<0.01$. White circles, Kv1.3 ($n=13$); black circles, Kv1.3-KCNE4 ($n=8$). (D) Representative traces for cumulative inactivation of outward K⁺ currents through Kv1.3 (left) or Kv1.3-KCNE4 (right) channels. Currents were elicited by a train of 25 × 200 millisecond depolarizing pulses to +60 mV once every 400 milliseconds. (E) Cumulative inactivation of Kv1.3 (white circles, $n=10$) and Kv1.3-KCNE4 (black circles, $n=5$) channels. The ratio of the peak current amplitude during each pulse, relative to that during the 1st pulse (I/I_{max}), is plotted against the time every pulse was applied. $\#P<0.001$. (F) Representative traces illustrating inactivation kinetics of Kv1.3 and Kv1.3-KCNE4 channels, in response to a 5 seconds depolarizing pulse to +60 mV. Time constant for inactivation ($\tau_{\text{inactivation}}$), obtained after fitting the data to a single exponential, were (in seconds): for Kv1.3 channels, 1.12 ± 0.2 ($n=10$); for Kv1.3-KCNE4 channels, 0.54 ± 0.08 ($n=6$; $P<0.05$).

Tomaselli, 2002; McCrossan et al., 2009). Therefore, we analyzed whether KCNE4 associates with Kv1.3. Fig. 2 demonstrates that KCNE4, but not KCNE2, retained Kv1.3 intracellularly. As we previously described (Vicente et al., 2008), Kv1.3 was targeted to the cell surface (Fig. 2A). Although KCNE2 distribution was similar to that of Kv1.3 (Fig. 2B), KCNE4 showed intracellular retention

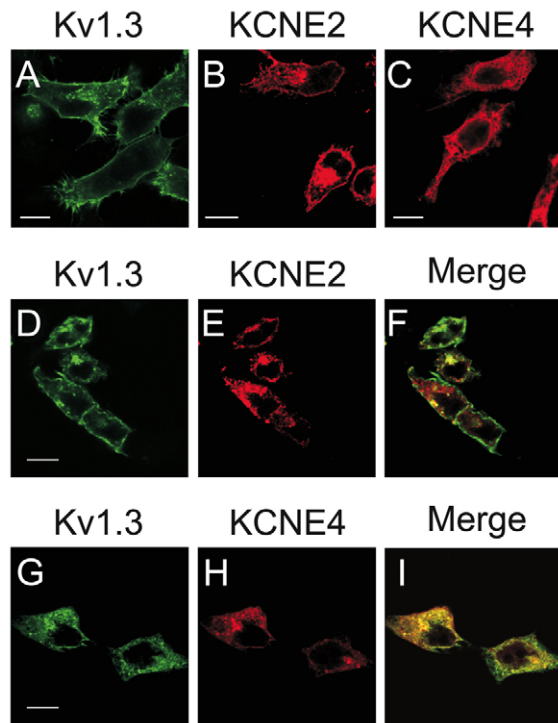


Fig. 2. Kv1.3 colocalizes with KCNE4. HEK293 cells were transiently transfected with Kv1.3-YFP (A), KCNE2 (B) or KCNE4 (C). Note that whereas Kv1.3 and KCNE2 have a robust surface membrane distribution, KCNE4 shows more intracellular retention. (D-I) Coexpression of Kv1.3 (D,G) with either KCNE2 (E) or KCNE4 (H). (F,I) Merged images of Kv1.3 and KCNE2, and Kv1.3 and KCNE4, respectively. Unlike KCNE2, KCNE4 triggers Kv1.3 intracellular retention. Scale bars: 10 μ m.

(Fig. 2C). Kv1.3, co-expressed with KCNE2, remained at the cell surface with minor colocalization (Fig. 2D-F). By contrast, when co-expressed with KCNE4, Kv1.3 localization changed and both proteins colocalized within intracellular compartments (Fig. 2G-I). Our results suggest an interaction between Kv1.3 and KCNE4, which alters channel localization.

Most KCNE ancillary subunits improve the membrane localization of their Kv partners (Li et al., 2006). However, we found a dominant negative effect. Therefore, we studied Kv1.3 surface membrane expression in the presence of KCNE4. Fig. 3 demonstrates that KCNE4, but not KCNE2, impairs Kv1.3 targeting to the plasma membrane, thereby diminishing the amount of protein at the surface. Indeed, Kv1.3 mostly colocalized with the plasma membrane marker WGA (Fig. 3A-D). The analysis in Fig. 3D, derived from the section indicated by a white arrow in Fig. 3C, indicated that both proteins mostly share the same location. KCNE peptides are targeted to the cell surface with different efficiencies (Um and McDonald, 2007; Jiang et al., 2009). In this context, KCNE2 (Fig. 3I-L), but not KCNE4 (Fig. 3E-H), colocalized with WGA. When KCNE4 was co-transfected with Kv1.3 (Fig. 3M-P), KCNE4-induced Kv1.3 intracellular retention impaired Kv1.3-WGA colocalization (Fig. 3U). In addition, Kv1.3 and KCNE4 did not colocalize at the cell surface. In contrast, KCNE2 did not modify Kv1.3 colocalization with WGA at the plasma membrane (Fig. 3Q-T,V). By using ImageJ software for a pixel-by-pixel analysis we found that 60% less KCNE4 was expressed at the cell surface than Kv1.3 and KCNE2. Unlike KCNE2, KCNE4 impaired Kv1.3

surface expression by 40% (Fig. 3W). KCNE4-CFP intracellular retention was not due to the fusion with CFP because KCNE4-HA showed a similar behavior (not shown). We further analyzed the amount of Kv1.3 at the cell surface by biotinylation in the presence of KCNE4. Fig. 4 shows that Kv1.3 is detected at the membrane as early as 4 hours following transfection. However, Kv1.3-KCNE4 and KCNE4 were detected after 12 and 24 hours, respectively. Therefore, KCNE4 delayed Kv1.3 reaching the cell surface (Fig. 4A). In addition, the amount of Kv1.3-KCNE4 at the membrane was tenfold less than Kv1.3 (Fig. 4B).

We have described that Kv1.3 exits the endoplasmic reticulum (ER) efficiently, which allows rapid sorting into Golgi vesicles designated for plasma membrane targeting. However, heteromeric association with Kv1.5 impairs Kv1.3 trafficking and increases ER retention (Vicente et al., 2008). Therefore, we wanted to study whether KCNE4-induced Kv1.3 retention was also associated with ER retention. Kv1.3 did not colocalize with an ER marker (Fig. 5A-C). However, KCNE4 was mostly targeted to this compartment (Fig. 5D-F). Thus, KCNE4 functions to retain Kv1.3 within the ER (Fig. 5G-J).

Oligomeric assembly of Kv1.3 and KCNE4

Although electrophysiological and confocal studies suggested an interaction between Kv1.3 and KCNE4, no physical association has been demonstrated. To this end, we designed a series of co-immunoprecipitation studies with differently tagged Kv1.3 and KCNE4 proteins. Fig. 6 demonstrates that KCNE4 forms a stable oligomer with Kv1.3. By co-transfecting KCNE4-CFP (~50 kDa) and Kv1.3-HA (~70 kDa) we found that Kv1.3 associated with KCNE4 (Fig. 6A,B). By contrast, no interaction was observed with KCNE2 (Fig. 6C). Thus, immunoprecipitation with an anti-Kv1.3 antibody against Kv1.3-YFP (~100 kDa) did not reveal an apparent KCNE2-CFP signal (~45 kDa). To unequivocally demonstrate that KCNE4 interacts physically with Kv1.3 we performed FRET experiments (Fig. 6D-G). As shown in Fig. 6H, FRET analysis revealed that a homomeric association between Kv1.3-YFP and Kv1.3-CFP gave a FRET signal greater than 20%. In this context, the oligomeric association of KCNE4-Kv1.3 resulted in ~15% significant FRET.

KCNE modulates Kv surface expression but the cellular compartment where this association takes place is uncertain. However, Kv β ancillary subunits form stable complexes with Kv1 channels in the ER (Nagaya and Papazian, 1997). Therefore, we next analyzed whether KCNE4 and Kv1.3 associate in this compartment. Brefeldin A (BFA) is an inhibitor of protein transport from the ER to the Golgi apparatus. The incubation of Kv1.3-KCNE4 HEK293 cells with BFA demonstrated that both proteins showed ER localization, which is upstream of the Golgi network and subsequent membrane targeting. Our results suggest that Kv1.3 and KCNE4 interact early in the secretory pathway in the ER, similar to what has been described with classical Kv β (Nagaya and Papazian, 1997). In addition, FRET experiments on living cells (Fig. 6G) further supported the molecular proximity of Kv1.3 and KCNE4 within the ER.

KCNE4 modifies Kv1.3 membrane surface targeting

The localization of Kv channels in specific locations at the plasma membrane leads to precise signaling and spatial compartmentalization. The composition of raft microdomains is crucial for Kv1.3 activity, thereby modulating immune responses. Kv1.3 localizes in lipid raft microdomains and cell activation

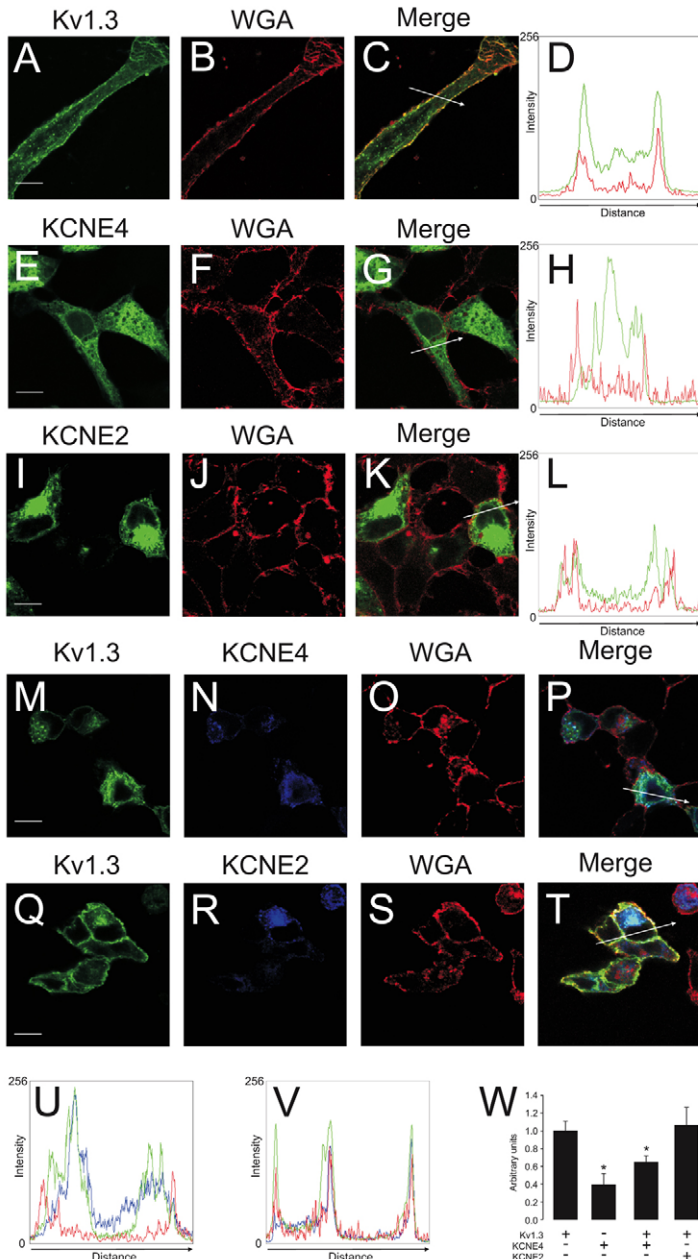


Fig. 3. KCNE4 impairs Kv1.3 targeting to the plasma membrane. Confocal images demonstrating that the presence of KCNE4 mistargets Kv1.3 surface expression, as analyzed by WGA overlay. (A-D) Kv1.3 shows membrane surface expression. (A) Kv1.3, (B) WGA, (C) merged image and (D) histogram of the pixel by pixel analysis of the section indicated by the arrow in C. Green, Kv1.3; red, WGA. (E-H) KCNE4 does not colocalize with WGA. (E) KCNE4, (F) WGA, (G) merged image and (H) histogram of the pixel by pixel analysis of the section indicated by the arrow in G. (I-L) KCNE2 shows strong colocalization with WGA. (I) KCNE2, (J) WGA, (K) merged image and (L) histogram of the pixel by pixel analysis of the section indicated by the arrow in K. (M-P) Coexpression of Kv1.3 and KCNE4. (M) Kv1.3, (N) KCNE4, (O) WGA and (P) merged image. Unlike in C, no Kv1.3 and WGA colocalization is observed. By contrast, massive Kv1.3 and KCNE4 colocalization is apparent (cyan). (Q-T) Coexpression of Kv1.3 and KCNE2. (Q) Kv1.3, (R) KCNE2, (S) WGA and (T) merged image. Unlike in P, Kv1.3 and WGA colocalize (yellow). Little triple colocalization (in white) is observed. (U,V) Histogram of the pixel by pixel analysis of the section indicated by the arrows in P and T, respectively. Green, Kv1.3; blue, KCNE2 or KCNE4; red, WGA. Although the presence of KCNE2 does not mistarget Kv1.3 to the surface (V), KCNE4 affects Kv1.3 and WGA colocalization (U). (W) Analysis of the relative expression of Kv1.3, KCNE4, Kv1.3-KCNE4 and Kv1.3-KCNE2. Pixel by pixel intensities from confocal images were analyzed using ImageJ software and compared with the relative intensity of Kv1.3 at the plasma membrane (determined by colocalization with WGA). Values are the mean \pm s.e.m. of at least 20 cells. * P <0.05 vs Kv1.3 (Student's t -test). Scale bars: 10 μ m.

concentrates Kv1.3 in lipid rafts near to signaling molecules (Panyi et al., 2004b). However, Kv1.3 targeting is impaired by oligomerization with Kv1.5 (Martinez-Marmol et al., 2008; Vicente et al., 2008). In addition, the association of Kv1.5 with the Kv β 2.1 regulatory subunit impairs channel targeting to rafts (Martinez-Marmol et al., 2008). With this in mind, we analyzed whether KCNE4 modifies Kv1.3 targeting to these domains. Although limited, Kv1.3-KCNE4 complexes reached the membrane surface (Fig. 4). Fig. 7 demonstrates that KCNE4 impaired Kv1.3 localization in lipid rafts. Although Kv1.3 targeted to rafts, KCNE4 did not localize to these domains (Fig. 7A,B). In Kv1.3-KCNE4 cells, Kv1.3 did not colocalize with caveolin, demonstrating that KCNE4 association mistargets Kv1.3 location (Fig. 7C). In addition, confocal microscopy experiments using FITC-labeled cholera toxin β subunit (CTX β), which is a marker

for rafts, further supports this result (Fig. 7D). In Kv1.3-KCNE4 cells the toxin did not colocalize with the hetero-oligomer (upper cell), in Kv1.3 cells, CTX β colocalized with the channel (lower cell).

To further investigate whether Kv1.3 homo- and Kv1.3-KCNE4 hetero-oligomers target to different membrane surface microdomains, we performed FRAP experiments (Fig. 8). Fluorescence recovery within membrane regions was monitored until a steady state was achieved. Mobile fractions were similar ($63 \pm 1\%$ and $65 \pm 1\%$ for Kv1.3 and Kv1.3-KCNE4, respectively) but the time constant ($t_{1/2}$) of the Kv1.3-KCNE4 hetero-oligomer exhibited greater lateral mobility (24 ± 2.1 seconds and 13 ± 1.7 seconds for Kv1.3 and Kv1.3-KCNE4, respectively, P <0.001). Our results indicate that KCNE4 association targets Kv1.3 to different membrane domains with higher mobility.

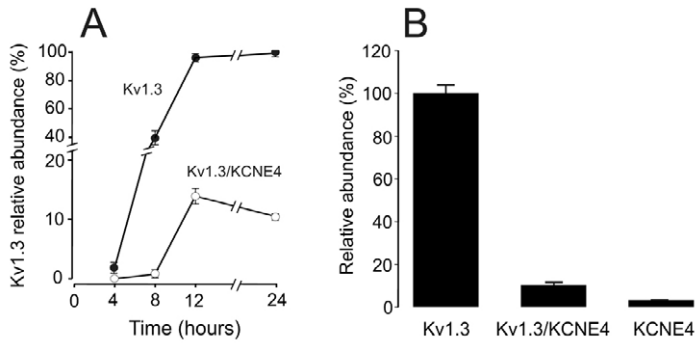


Fig. 4. KCNE4 delays and diminishes the expression of Kv1.3 at the cell surface. (A) HEK293 cells were transiently transfected with Kv1.3-YFP, KCNE4-CFP and Kv1.3-YFP/KCNE4-CFP. After transfection, cells were labeled with biotin at different times and processed as described in Materials and Methods. Western blot analysis was performed with and anti-GFP antibody. Values are means \pm s.e.m. ($n=4$) of the percentage of the biotinylated surface protein relative to the maximal expression of Kv1.3. black symbols, Kv1.3; white symbols, Kv1.3-KCNE4. (B) Relative abundance (%) of biotinylated proteins compared with Kv1.3 after 24 hours of transfection. Values are means \pm s.e.m. ($n=4$) of the percentage of the biotinylated surface protein relative to the expression of Kv1.3 24 hours post-transfection. Note that Kv1.3-KCNE4 is about 10 times less abundant than Kv1.3 alone.

Macrophages express Kv1.3 and KCNE4

Our results thus far indicate important physiological significance. Kv1.3 is involved in macrophage physiology and the expression of Kv1.3 and putative partners, such as Kv1.5 and Kv β subunits, is under extensive regulation (Vicente et al., 2005; Vicente et al., 2006). In addition, Kv channels in leukocytes are considered pharmacological targets (Wulff et al., 2003; Beeton and Chandy, 2005) and the composition of the channel complex could impair potential therapies (Villalonga et al., 2007). Therefore, differential regulation of Kv1.3 and KCNE4 could modify the subunit composition of the channel, altering their biophysical and physiological properties. KCNE4 and Kv1.3 mRNAs were expressed in RAW 264.7 macrophages (Fig. 9A). This coexpression is a general characteristic of leukocytes because Jurkat T cells also share this phenotype (not shown). Unfortunately, unlike Kv1.3, we were not able to detect KCNE4 in macrophages by western blot with commercially available antibodies (not shown). Similarly, immunocytochemistry studies with anti-Kv1.3 and anti-KCNE4 antibodies were unsuccessful. However, because RAW cells have Kv1.3 and KCNE4 intracellular processing and trafficking programs, we transfected these cells with Kv1.3-YFP and KCNE4-CFP. In general, cells were poorly transfected, but confocal microscopy analysis of double-transfected RAW cells demonstrated that KCNE4 colocalizes with Kv1.3 in macrophages (Fig. 9B,C). In addition, although Kv1.3 is targeted to the plasma membrane (Fig. 9B), the presence of KCNE4 impaired Kv1.3 targeting (Fig. 9C).

Our data suggest that KCNE4 functions as a Kv1.3 negative modulatory subunit. Therefore, the regulation of KCNE4 might affect channelosome composition triggering important physiological consequences. For this reason, we analyzed the regulation of

KCNE4 and Kv1.3 upon activation and immunosuppression in macrophages. Lipopolysaccharide, which activates macrophages and regulates Kv (Vicente et al., 2003), increased Kv1.3 and KCNE4 mRNA expression up to three- and 12-fold, respectively (Fig. 9D). By contrast, the addition of dexamethasone (DEX) for 24 hours decreased Kv1.3 by 50% with no effects on KCNE4.

Discussion

This study demonstrates that Kv1.3 and KCNE4 form oligomeric structures and suggests that KCNE4 might act as an inhibiting ancillary subunit for the Kv channel in macrophages. Furthermore, our data show that their association leads to biophysically distinct channels. The present report also demonstrates, for the first time, that KCNE peptides associate with members of the Kv1 (Shaker) family and alters channel surface expression and trafficking. This association further increases the number of possible oligomeric combinations of the Kv channelosome in leukocytes. Thus, similar to nervous tissue and muscles, it is difficult to assign currents to specific channels in the immune system.

Electrophysiological studies suggested that lymphocytes express several Kv channels (n -, n' - and l -type). Kv1.3 was associated with the n -type channel whereas the l -type was attributed to Kv3.1 (Grissmer et al., 1990; Grissmer et al., 1992). However, the protein responsible for the n' -type is largely unknown, although other channels, such as Kv1.1, Kv1.2, Kv1.5 and Kv1.6, have been described in immune-system cells (Freedman et al., 1995; Jou et al., 1998; Liu et al., 2002; Vicente et al., 2003; Mullen et al., 2006). Therefore, currents might be accounted for by a variety of hybrid forms and heteromeric formation of K⁺ channels has been suggested as mechanisms to increase channel functional diversity (Manganas and Trimmer,

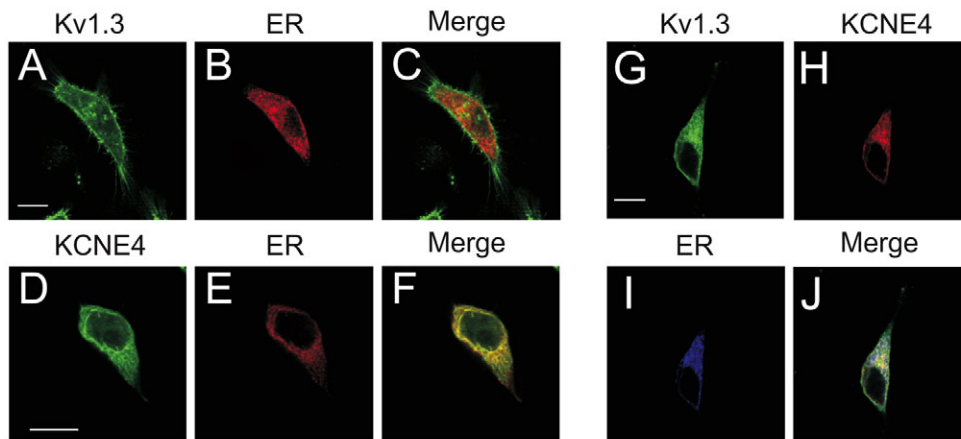


Fig. 5. KCNE4 retains Kv1.3 at the endoplasmic reticulum. Kv1.3-YFP and KCNE4-CFP have distinct cellular distributions. HEK293 cells were transiently transfected with Kv1.3-YFP, KCNE4-CFP, Kv1.3-YFP/KCNE4-CFP and DsRed-ER marker. (A-C) Kv1.3 does not colocalize with the ER. (D-F) KCNE4 shows strong ER colocalization. (A,D) Kv1.3 and KCNE4 respectively; (B,E) DsRed-ER marker; (C,F) merged image of Kv1.3- and KCNE4-transfected cells respectively. Yellow indicated colocalization. (G-J) Coexpression of Kv1.3, KCNE4 and DsRed-ER marker. (G) Kv1.3; (H) KCNE4; (I) DsRed-ER marker; (J) merged image. White color indicates triple colocalization. Scale bars: 10 μ m.

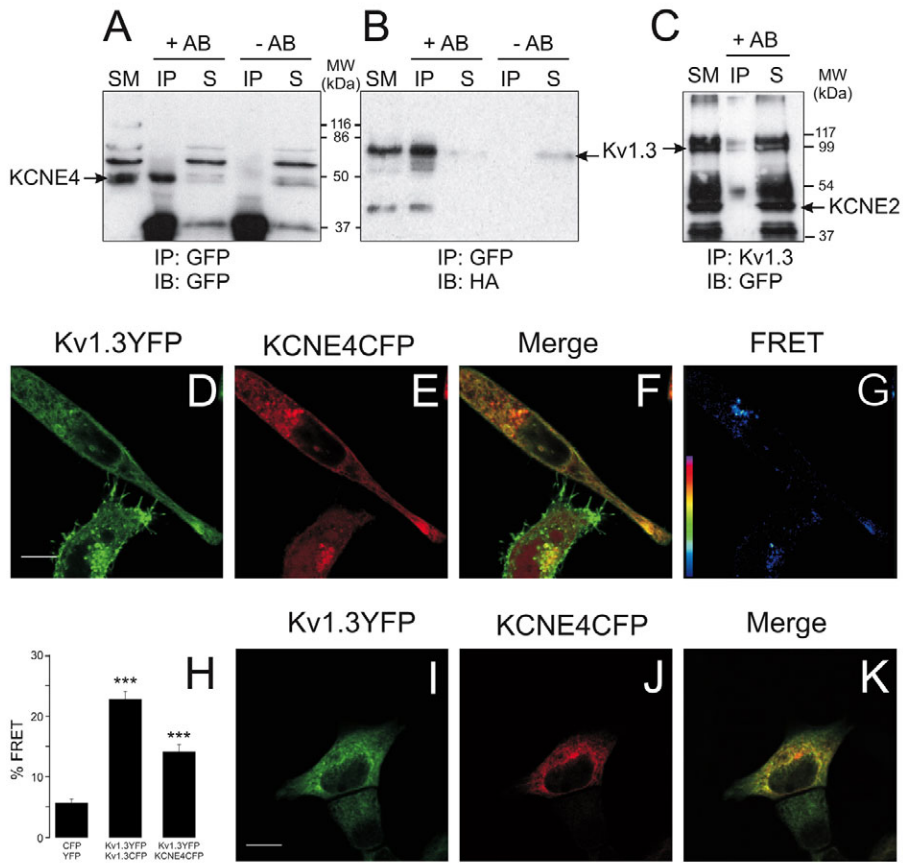


Fig. 6. KCNE4 associates with Kv1.3. KCNE4, but not KCNE2, and forms stable complexes with Kv1.3. (A,B) HEK293 cells were transiently transfected with Kv1.3-HA and KCNE4-CFP. Cells were lysed and total cell extracts were immunoprecipitated with anti-GFP antibody. (A) Western blot against GFP demonstrating that KCNE4-CFP immunoprecipitates. (B) Western blot against HA demonstrating that Kv1.3-HA co-immunoprecipitates with KCNE4-CFP. (C) KCNE2 does not interact with Kv1.3. HEK293 cells were transiently transfected with Kv1.3-YFP and KCNE2-CFP. Cells were lysed and total cell extracts were immunoprecipitated with anti-Kv1.3 antibody. Western blot against GFP demonstrates that Kv1.3 does not co-immunoprecipitate with KCNE2. SM, starting material; IP, immunoprecipitate; S, immunoprecipitate supernatant; +AB, immunoprecipitation in the presence of antibody; -AB, immunoprecipitation in the absence of antibody. (D-H) Representative fluorescence resonance energy transfer (FRET) experiment. Panels show fluorescence signal of Kv1.3-YFP and KCNE4-CFP. (D) Kv1.3; (E) KCNE4; (F) merged image; (G) FRET channel. FRET shows the YFP fluorescence intensity after CFP excitation. (H) Histogram shows FRET efficiency of different combinations of proteins. Negative control was performed with cells expressing CFP and YFP. Positive control was performed using cells expressing Kv1.3-CFP and Kv1.3-YFP. ****P* < 0.001 vs CFP/YFP (*n* = 10, Student's *t*-test). (I-K) Kv1.3 and KCNE4 associate in the ER. HEK293 cells were doubly transfected with Kv1.3-YFP (green) and KCNE4-CFP (red) and brefeldin A was added to the culture. (I) Kv1.3; (J) KCNE4; (K) Merged image shows colocalization (yellow). Scale bars: 10 μ m.

2000; Vicente et al., 2006). This complexity might be further increased by the presence of auxiliary subunits, such as Kv β , which confers rapid inactivation, alters current amplitude and gating, and promotes Kv cell surface expression (Manganas and Trimmer, 2000). In fact, Kv1.3 is able to assemble with Kv β subunits to form functional Kv channels, increasing the variety of electrical responses in leukocytes. The expression of Kv1.3 together with Kv β subunits modifies the rate of inactivation and the amplitude of the K⁺ current (McCormack et al., 1999). Although Kv β 1 peptides accelerate the rate of inactivation, Kv β 2 mostly facilitates surface expression (Martens et al., 1999;

Manganas and Trimmer, 2000). Surprisingly, KCNE4 controls both fast inactivation and plasma membrane expression.

KCNE regulatory subunits have been primarily studied in the heart but their activity in the brain and in many other tissues is being increasingly recognized (McCrossan and Abbott, 2004). KCNE peptides associate with Kv7.1 and Kv11.1 channels generating cardiac *I*_{ks} (slowly activating delayed rectifier K⁺) and *I*_{kr} (rapid delayed rectifier K⁺) currents (Barhanin et al., 1996; Abbott et al., 1999). However, KCNE shows more promiscuity than previously thought. For example, KCNE3 in association with Kv3.4 sets resting membrane potential in skeletal muscle cells

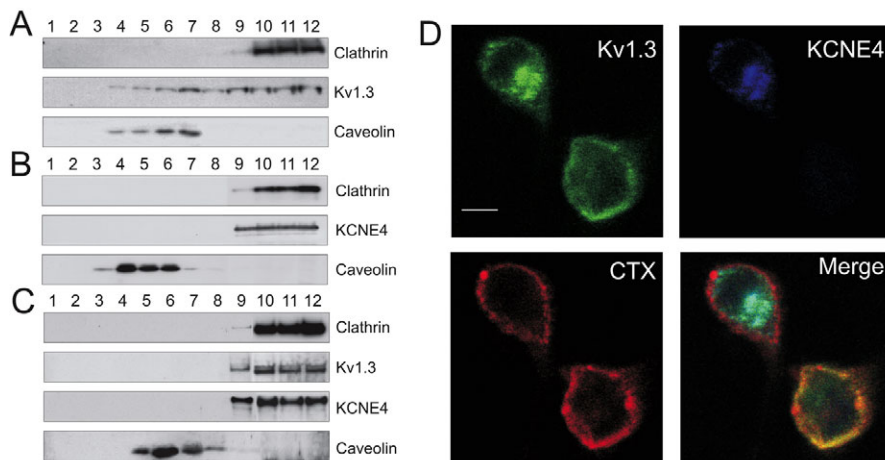


Fig. 7. KCNE4 impairs Kv1.3 localization in lipid rafts. Unlike KCNE4 and Kv1.3-KCNE4 hetero-oligomers, Kv1.3 channels target to lipid rafts. (A-C) Detergent-based isolation of lipid rafts. Sucrose density gradient centrifugation of 1% Triton-X-100-solubilized extracts from cells, transfected with Kv1.3 (A), KCNE4 (B) or doubly-transfected with Kv1.3 and KCNE4 (C) were analyzed by western blot. Caveolin indicates low-buoyancy rafts, but clathrin is found in non-floating fractions. Lane numbers denote different fractions from the top (1) to the bottom (12) of the sucrose density gradient. (D) KCNE4 association impairs Kv1.3 colocalization with FITC-labeled cholera toxin β subunit (CTX β). Green, Kv1.3; blue, KCNE4; red, CTX β ; merged image, yellow represents colocalization between Kv1.3 and CTX β in a KCNE4-negative cell (bottom cell). Top cell is a KCNE4-positive cell that shows no colocalization between Kv1.3 and CTX β . Cyan represents Kv1.3-KCNE4 colocalization. Scale bar: 5 μ m.

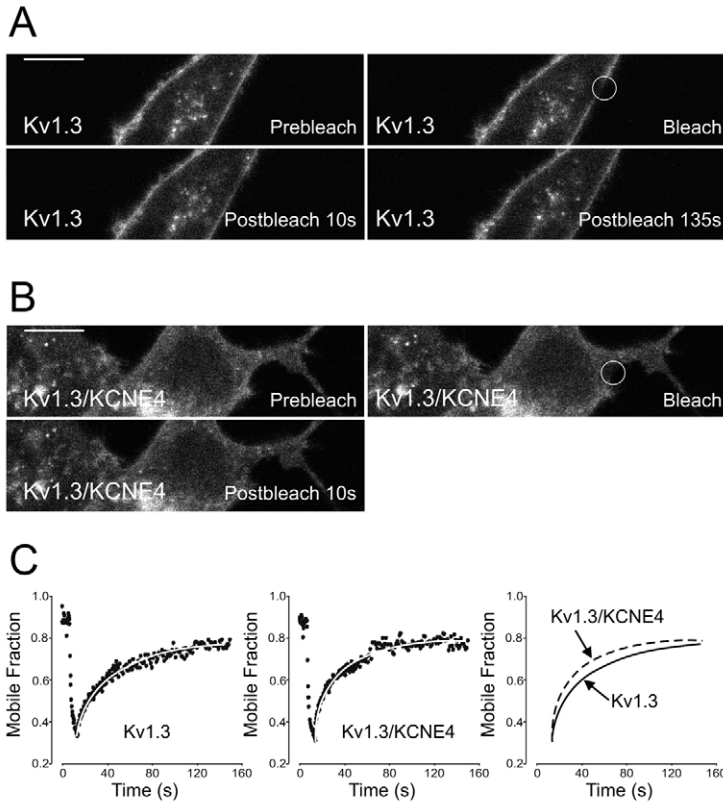


Fig. 8. Fluorescence recovery after photobleaching (FRAP) of Kv1.3 and Kv1.3-KCNE4. FRAP experiments monitored YFP intensity after 20 iterations of bleaching with 100% laser power. Representative images of Kv1.3-YFP at different times. Circles indicate regions of interest. (A) Kv1.3; (B) Kv1.3-KCNE4. Scale bars: 10 μ m. (C) Graphs of the average ($n=10$) intensity from Kv1.3 and Kv1.3-KCNE4. Right, Kv1.3; center, Kv1.3-KCNE4; left, the regression analysis of the data (white lines from Kv1.3 and Kv1.3-KCNE4 panels) for comparison. Solid line, Kv1.3; Dashed line, Kv1.3-KCNE4.

(Abbott et al., 2001). In addition, KCNE1 and KCNE2 form stable complexes with Kv2.1 in the heart and brain (McCossan et al., 2009). Few studies have demonstrated the existence of KCNE in leukocytes. KCNE1 was cloned from T-cells (Attali et al., 1992) and the KCNE3 and KCNE4 have been detected in leukocytes (Grunnet et al., 2003; Lundquist et al., 2006). We have found that KCNE4 is present in macrophages and T-cells (not shown). In addition, similarly to Kv1.3, lipopolysaccharide-induced activation increases KCNE4; and in cells treated with DEX, Kv1.3 is downregulated but KCNE4 remains constant. This behavior is in agreement with a putative negative regulatory action of KCNE4. Whereas pro-inflammatory agents, such as lipopolysaccharides, activate leukocytes (Vicente et al., 2003), prolonged insult triggers cell death by apoptosis (Detre et al., 2006). In this context, Kv1.3 seems to play a dual role. The channel is involved in the initiation of the signaling, but it also contributes to programmed cell death (Panyi et al., 2004a; Szabo et al., 2008). Sustained Kv1.3 induction would be downregulated by an increase in KCNE4 and the formation of Kv1.3-KCNE4 oligomers. In this scenario, lower expression, or repression, of Kv1.3 makes the cell resistant to apoptosis (Szabo et al., 2008). Therefore, the formation of Kv1.3-KCNE4 complexes would fine-tune the cell response. However, under an immunosuppressant insult, such as DEX, the dominant-negative effect of KCNE4 will have no physiological relevance.

KCNE4 specifically decreases Kv1.3 currents concomitantly with a reduction in channel surface expression and traffic. In addition, activation, C-type inactivation and cumulative inactivation are altered by KCNE4. Apart from cardiac Kv7.1 and Kv11.1, a number of different channels are affected by KCNE peptides (McCossan and Abbott, 2004). For instance, KCNE1 slows Kv3.1 and Kv3.2 activation and KCNE3 increases the activation time constants of Kv2.1, Kv3.1 and Kv3.2 (McCossan et al., 2003;

Lewis et al., 2004). In addition, KCNE3 also modulates Kv3.4 current without a significant effect on either Kv1.4 or Kv4.1 (Abbott et al., 2001). Grunnet et al. demonstrated that among all KCNE peptides, only KCNE4 is able to modify Kv1.3 currents (Grunnet et al., 2003). Unlike other KCNE members, KCNE4 could act as a repressor ancillary subunit because unrelated channels such as Kv7.1 and the calcium and voltage-gated $K_{Ca}1.1$ channel (BK) are also inhibited by KCNE4 (Grunnet et al., 2002; Levy et al., 2008). It is important to point out that unlike other KCNE proteins, KCNE4 possesses a larger C-terminal intracellular domain (McCossan and Abbott, 2004; Rocheleau et al., 2006). It is tempting to speculate that this bulky domain is involved in these processes but this hypothesis warrants further research. However, the inhibitory property of KCNE4 on selected channels, such as Kv7.1, seems to be very efficient as well as specific because Kv7.2 to Kv7.5 and Kv11.1 channels are unaffected (Grunnet et al., 2002).

To what extent electrophysiological changes have functional relevance is not known. As previously described, most ancillary subunit modulation might not be physiologically relevant (Deschenes and Tomaselli, 2002). Our results suggest that this is not the case for Kv1.3 and KCNE4 in leukocytes. Changes in trafficking and surface expression in macrophages further support Kv1.3-KCNE4 oligomeric channels, and Kv1.3 spatial regulation points towards a specific and physiological interaction. Other KCNE interactions with Kv1 members (Shaker) have been documented. Thus, KCNE1 and KCNE2 associate with Kv1.5, and experiments with *kcne2* null mice suggest that associations with Kv1.5 and Kv4.2, but not with Kv1.4 and Kv4.3, recapitulate cardiac I_{Kslow} and $I_{to,f}$ (transient outward fast) currents (Melman et al., 2004; Roepke et al., 2008).

KCNE peptides also control the surface expression of K^+ channels (McCossan and Abbott, 2004). In addition, specific

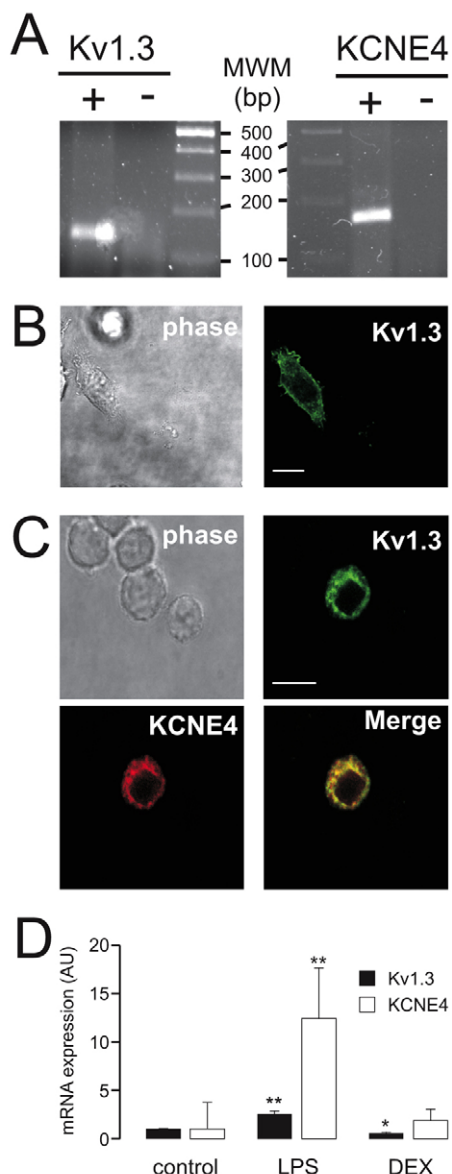


Fig. 9. RAW 264.7 macrophages express Kv1.3 and KCNE4. (A) Kv1.3 and KCNE4 mRNA expression analyzed by RT-PCR. Total RNA was extracted from RAW macrophages and PCR reactions were performed in the presence (+) or the absence (-) of the retrotranscriptase reaction. (B,C) KCNE4 impairs Kv1.3 targeting to the macrophage membrane and increases intracellular retention. (B) Kv1.3 expression. Right, phase image of a RAW macrophage. Left, confocal imaging of Kv1.3-YFP in the same cell. (C) Kv1.3-KCNE4 expression. Upper left, phase image of RAW macrophages; upper right, a cell expressing Kv1.3-YFP; lower left, KCNE4-CFP expression in the same cell; lower right, merged image showing colocalization in yellow. Note that in macrophages that expressed both proteins, Kv1.3 was mostly intracellular. Scale bar, 10 μ m. (D) Kv1.3 and KCNE4 are differentially regulated upon activation and immunosuppression. Cells were incubated for 24 hours in the presence or the absence of lipopolysaccharides (LPS) and DEX. Samples were collected and Kv1.3 and KCNE4 mRNA expression was analyzed by real-time PCR. Black bars, Kv1.3; white bars, KCNE4. Values are the means \pm s.e.m. of the relative mRNA expression ($n=4$). Significant differences were found in the presence of lipopolysaccharides (Kv1.3: * $P < 0.05$ and ** $P < 0.01$ vs control and KCNE4: ** $P < 0.01$ vs control; Student's t -test) and DEX (Kv1.3: * $P < 0.05$ vs control, Student's t -test). Relative mRNA was calculated using standard curves, and fold variation in arbitrary units (AU) were normalized to the relative quantity (RQ) of 18S as follows: (Kv1.3 or KCNE4 RQ at 24 hours/18S RQ at 24 hours)/(Kv1.3 or KCNE4 RQ at control/18S RQ at control).

associations are crucial for KCNE1 expression at the plasma membrane (Chandrasekhar et al., 2006). In fact, KCNE1 shows greater ER retention than KCNE2 and this determines Kv11.1 association (Um and McDonald, 2007). KCNE4 also shows more ER retention than KCNE2. Although KCNE4 and KCNE2 share an intracellular RR motif, KCNE4 possess multiple arginine and lysine-based ER retention signals (Sharma et al., 1999; Michelsen et al., 2005; Zuzarte et al., 2009). KCNE4 does not modify surface expression of Kv7.1 and Kv1.1 (Grunnet et al., 2002; Grunnet et al., 2003). However, both channels exhibit less surface expression than Kv1.3. In addition, the cellular compartment where KCNE associates with K^+ channels is controversial. Although some studies demonstrate that, unlike Kv β subunits, this interaction takes place at the membrane (Grunnet et al., 2002), others indicate an association in the ER (Krumer et al., 2004; Chandrasekhar et al., 2006). Our results indicate that, similar to Kv β , KCNE4 associates with Kv1.3 in the ER.

Besides trafficking, lipid raft sublocalization regulates ion channels by compartmentalizing signaling components. Kv1.3 targets to different rafts upon activation and apoptosis in lymphocytes (Szabo et al., 2004; Vicente et al., 2008). Disruption of these domains alters channel activity and raft association seems to be dynamic because the interaction with other subunits, such as Kv1.5, impairs this localization (Vicente et al., 2008). However, scaffolding proteins, such as membrane associated guanylate kinases (MAGUK) and caveolins, improve Kv1.5 channel association with raft domains (Folco et al., 2004). Unlike scaffolding proteins, Kv β 2.1 regulatory subunit mistargets Kv1.5 channels to lipid rafts (Martinez-Marmol et al., 2008). Similarly, KCNE4 act as a repressor ancillary subunit. Kv1.3 localizes in rafts but this is strongly dependent on associations with KCNE4. Because Kv1.3 activity is regulated by the composition of the lipid raft (Szabo et al., 2004), different membrane platform locations must be contemplated as an important regulatory mechanism of Kv1.3 in leukocyte physiology. The channelosome composition is a determinant in shaping the repertoire of Kv1.3 channels present at the plasma membrane of leukocytes. This composition affects the expression and functional properties of the channels and contributes to the diversity of K^+ channels in leukocytes. This data will be critical for further determination of the molecular composition of individual Kv currents and the physiological relevance of these α - β interactions. Investigation of the mechanisms involved in the regulation of potassium ion conduction is, therefore, essential for understanding potassium channel function in the immune response to infection and inflammation. Macrophages turn the immune response toward inflammation or tolerance. These cells, which also act as antigen-presenting cells, modify the cytokine milieu and the intensity of T-lymphocyte signaling. In response to different growth factors and cytokines, macrophages can proliferate, become activated or differentiate. These cells have a key function at inflammatory loci, where they remain until inflammation disappears. However, the persistence of activated macrophages at inflammatory loci is associated with a wide range of inflammatory diseases. The negative KCNE4 effect on Kv1.3 could be interpreted in this life-time scenario.

In summary, Kv1.3 trafficking, targeting and activity are dramatically modified by the presence of KCNE4. The association of Kv1.3 and KCNE4, which are coexpressed in the immune system, could play a crucial role in controlling the immunological response. Therefore, our results further the understanding of how K^+ channels are involved in leukocyte physiology and indicate that KCNE4 could be a novel pharmacological target in the immune system.

Materials and Methods

Expression plasmids

rKv1.3 in pRCMV was provided by Todd C. Holmes (New York University, New York, NY). mKCNE4 in pSGEM was from Michael Sanguinetti (University of Utah, Salt Lake City, UT). hKCNE2 in pHA was obtained from Susana de la Luna (CRG, Barcelona, Spain). Kv1.3, KCNE4 and KCNE2 were subcloned into pEYFP-C1 (Kv1.3) and pECFP-N1 (KCNE2 and KCNE4; Clontech). Constructs were verified by sequencing. rKv1.3, externally tagged with HA between S3 and S4, was from Donald B. Arnold (University of Southern California, Los Angeles, CA). piRES-EGFP-hKCNE4-HA was obtained from Alfred L. George (Vanderbilt University, Nashville, TN). The endoplasmic reticulum marker, pDsRed-ER, was obtained from Clontech.

Cell culture and transient transfections

HEK293 cells were grown on poly-lysine-coated coverslips in DMEM containing 10% fetal bovine serum (FBS). Transient transfection was performed using MetafectenePro (Biontech) at nearly 80% confluence. Twenty-four hours after transfection, cells were washed in PBS (phosphate-buffered saline), fixed and mounted with Aqua Poly/Mount from Polysciences. In some experiments, Kv1.3-KCNE4-transfected cells were treated with 2.5 μ g/ml brefeldin A (BFA) for 12 hours.

RAW 264.7 macrophages were cultured in RPMI culture medium containing 5% FBS supplemented with 10 IU/ml penicillin and streptomycin, and 2 mM L-glutamine. Cells, grown in 100-mm tissue culture dishes, were incubated with lipopolysaccharides (100 ng/ml) and DEX (1 μ M; Sigma) for 24 hours. In some experiments, RAW cells were transfected with Kv1.3-YFP and KCNE4-CFP and processed as above.

RNA isolation, RT-PCR analysis and real-time PCR

Total RNA from RAW 264.7 macrophages was isolated using Nucleospin RNAII (Machery-Nagel). RNA was treated with DNase I and cDNA synthesis was performed using transcriptase reverse transcriptase (Roche) with a random hexanucleotide and oligo(dT) according to the manufacturer's instructions.

Real-time PCR was performed using a LightCycler machine (Roche) with LightCycler FastStart DNA Master^{PLUS} SYBR Green I (Roche), according to the manufacturer's instructions. PCR primers were: Kv1.3, F: 5'-AGTATATG-GTGATCGAAGAGG-3', R: 5'-AGTGAATATCTTCTTGATGTT-3' (136 bp); KCNE4, F: 5'-CCTGACAGAGAAGAGAAACA-3', R: 5'-TGAACAGCACATACCCAG-3' (139 bp). The reactions were performed under the following conditions: 95°C for 5 seconds, 55°C for 8 seconds, and 72°C for 9 seconds, proceeded by 10 minutes at 95°C and followed by 10 minutes at 95°C. Melting curves were performed to verify the specificity of the product and 18S (AN: X00686), F: 5'-CGAGAATTCCTCCGACCC-3', R: 5'-CCCAAGCTCCAACTACGAGC-3' (212 bp), was included as an internal reference, as previously described (Villalonga et al., 2007). Results were analyzed with Light Cycler software 3.5 (Roche). For each primer set, a standard curve was made and the slope factor calculated. Values were normalized to the corresponding 18S. The corresponding real-time PCR efficiency (E) of one cycle in the exponential phase was calculated according to the equation: $E = 10^{(-1/\text{slope})}$.

Protein extraction, co-immunoprecipitation and western blotting

Cells were washed twice in cold PBS and lysed on ice with lysis solution (1% Triton X-100, 10% glycerol, 50 mM Hepes pH 7.2, 150 mM NaCl) supplemented with 1 μ g/ml aprotinin, 1 μ g/ml leupeptin, 1 μ g/ml pepstatin and 1 mM phenylmethylsulfonyl fluoride as protease inhibitors. Homogenates were centrifuged at 3000 g for 10 minutes and the supernatant was divided into aliquots and stored at -20°C. Protein content was determined using the Bio-Rad Protein Assay (Bio-Rad).

For co-immunoprecipitation, samples were precleared with 25 μ l of protein G-Sepharose beads, for 2 hours at 4°C with gentle mixing. The beads were then removed by centrifugation at 1000 g for 30 seconds at 4°C. The sample was then incubated overnight with the desired antibody (4 ng/ μ g protein) at 4°C with gently mixing. 30 μ l of protein-G-Sepharose was added to each sample for 4 h at 4°C. The beads were removed by centrifugation at 1000 g for 30 seconds at 4°C, washed four times in PBS, and resuspended in 70 μ l of SDS sample buffer.

Protein samples (50 μ g) and immunoprecipitates were boiled in Laemmli SDS loading buffer and separated on 10% SDS-PAGE. Next, they were transferred to nitrocellulose membranes (Immobilon-P; Millipore) and blocked in 0.2% Tween-20-PBS supplemented with 5% dry milk, before immunoreaction. Filters were immunoblotted with antibodies against Kv1.3 (1/200, Alomone), HA (1/200, Sigma) and GFP (1/1000, Roche). Anti-pan-caveolin antibody, which recognizes caveolin 1, 2 and 3 was used as a marker of lipid raft fractions (1/1000; BD Transduction) and anti-clathrin antibody was used to characterize non-floating fractions (1/1000, Chemicon).

Raft isolation

Low density, Triton-insoluble complexes were isolated as previously described (Martens et al., 2000) from HEK293 cells transiently transfected with either Kv1.3-YFP or double transfected with Kv1.3-YFP and KCNE4-CFP. Cells were homogenized in 1 ml of 1% Triton X-100, and sucrose was added to a final concentration of 40%.

A 5-30% linear sucrose gradient was layered on top and further centrifuged (260,000 g) for 20-22 hours at 4°C in a Beckman SW41 rotor. Gradient fractions (1 ml) were collected from the top and analyzed by western blotting.

Confocal microscopy, FRET and FRAP

Staining with FITC-labeled cholera toxin β subunit (CTX β) for lipid raft microdomains and wheat germ agglutinin (WGA)-Texas red (Invitrogen) for the plasma membrane was performed under non-permeabilized conditions. Cells were washed with PBS at 4°C and stained with FITC-CTX β or WGA for 30 minutes at 4°C. Subsequently, cells were washed and fixed with 4% paraformaldehyde in PBS for 6 minutes.

Fluorescence resonance energy transfer (FRET) sensitized emission was used to measure the molecular proximity between Kv1.3 and KCNE4. A Leica TCS SL laser scanning confocal microscope (Leica Microsystems) equipped with an argon laser, 63 \times oil immersion objective lens (NA 1.32) and a double dichroic filter (458/514 nm) was used. CFP was used as the donor fluorochrome paired with YFP, as the acceptor fluorochrome. To measure FRET, three images were acquired in the same order in all experiments through (1) the CFP channel (absorption 458 nm; emission 465-510 nm), (2) the FRET channel (absorption 458 nm; emission 525-600 nm) and (3) the YFP channel (absorption 514 nm; emission 525-600 nm). The background values were subtracted from the image values before performing FRET calculations. Control and experimental images were taken under the same photomultiplier gain conditions, offset and pinhole aperture. In order to calculate and eliminate non-FRET components from the FRET channel, images of cells transfected with either CFP or YFP alone were taken under the same conditions as for the experiments. The fraction of cross-over of CFP (A) and YFP (B) fluorescence was calculated for the different experimental conditions. Corrected FRET (FRET^c) was calculated on a pixel-by-pixel basis for the entire image using the equation: $\text{FRET}^c = \text{FRET} - (A \times \text{CFP}) - (B \times \text{YFP})$, where FRET, CFP and YFP are the values for the background-subtracted images of cells expressing CFP and YFP acquired through the FRET, CFP and YFP channels, respectively. Mean FRET^c values were calculated from mean fluorescence intensities for each selected region of interest (ROI) according to the above equation, and normalized (FRET^N) values for membrane regions were calculated according to the following equation: $\text{FRET}^N = \text{FRET}^c / \text{YFP}$. All calculations were performed using the FRET sensitized emission wizard from Leica Confocal Software and Microsoft Excel. FRET values were expressed as the mean \pm s.e.m. of $n > 15$ cells for each group.

Fluorescence recovery after photobleaching (FRAP) experiments were performed 1 day after transfection at room temperature. Dishes were replaced every 2 hours. Time series were taken with 20 scans before bleaching, which was accomplished by 20 iterations of bleaching with 100% laser power of the 514 nm line followed by 100 scans every 0.36 seconds and 100 scans every second (2.5 minutes in total) of the bleached region with 6% laser power. In each cell, a circular ROI of 6.57 μ m² was bleached. Experiments were performed with $n > 15$ cells per group. Fluorescence intensity was normalized to the prebleach intensity. Any loss of fluorescence during the recording was corrected with unbleached regions of the cell. The mobile fraction (F_M) was calculated according to the following equation: $F_M = (F_\infty - F_1) / (F_0 - F_1)$, where F_∞ is the fluorescence at the end of the steady state, F_1 is the fluorescence intensity post-bleaching and F_0 is the fluorescence of the ROI previous to the bleaching.

Values were fitted to a non-linear regression equation, $F(t) = F_M [1 - \exp(-t/\tau_{1/2})]$, where F is the fluorescence intensity, F_M is the mobile fraction and $\tau_{1/2}$ is the time constant. Data are given as mean \pm s.e.m. Statistical analysis was performed using Student's t -test (GraphPad Prism).

Cells were examined with a 63 \times oil immersion objective on a Leica TCS SL laser scanning confocal microscope. All offline image analysis was done using Leica confocal and Image J software and Sigmaplot.

Biotinylation of cell surface proteins

Cell surface biotinylation was carried out with the Pierce Cell Surface Protein Isolation Kit (Pierce) following manufacturer's instructions. HEK293 cells were transfected with Kv1.3-YFP, KCNE4-CFP or both constructs and their temporal presence at the surface was analyzed by western blotting. At the desired times after transfection, cell surface proteins were labeled with sulfo-succinimidyl-2-(biotinamido)ethyl-1,3-dithiopropionate (Sulfo-NHS-SS-biotin; Pierce). Briefly, cells were washed with ice-cold PBS twice, and Sulfo-NHS-SS-biotin was added and incubated at 4°C with constant rotation for 30 minutes. Excess biotin was quenched with quenching solution. Cells were treated with lysis buffer and centrifuged at 10,000 g for 2 minutes at 4°C. Clear supernatant was reacted with immobilized NeutrAvidin gel slurry in columns (Pierce) to isolate surface proteins. Columns were washed and protein eluted in sample buffer containing DTT. Surface proteins were resolved on a SDS-PAGE gel and the samples were analyzed by western blotting using a monoclonal anti-GFP antibody (Roche). Western blot bands were quantified using Phoretix (Nonlinear Dynamics). Data are expressed as the optical density (%) of the biotinylated protein relative to the maximal expression of Kv1.3. Filters were also immunoblotted with β -actin monoclonal antibody (Sigma) as control.

Electrophysiology

Whole-cell currents were measured with a D-6100 Darmstadt amplifier (List Medical) using the patch clamp technique. Currents were low-pass filtered at 1 kHz. Series resistance compensation was always above 70%. The pClamp8 software (Axon

Instruments) was used for pulse generation and data acquired using an Axon Digidata A/D interface and subsequent analysis. Electrodes were fabricated from borosilicate glass capillaries (Clark Electromedical Instruments) using a Flaming-Brown (P-87) micropipette puller (Sutter Instruments) and fire polished. Pipettes had a resistance of 2–3 M Ω when filled with a solution containing (in mM): 144 KCl, 0.2 CaCl₂, 1.2 MgCl₂, 10 Hepes, 0.5 EGTA (pH 7.35 and 302 mosmoles/l). The extracellular solution contained (in mM): 150 NaCl, 4 KCl, 2 CaCl₂, 1 MgCl₂, 10 Hepes (pH 7.4 and 310 mosmoles/l). Cells were clamped to a holding potential of –80 mV. To evoke voltage-gated currents, all cells were stimulated with 200-millisecond square pulses ranging from –100 to +60 mV in 20 mV steps. All recordings were routinely subtracted for leak currents. To calculate inactivation time constants (τ), cells were held at –80 mV and a +60 mV pulse potential of 5 seconds was applied. Inactivation adjustment was calculated from the peak of the current at 60 mV to the steady-state inactivation, and traces were fitted with Sigma Plot (SPSS, Chicago, IL). To analyze cumulative inactivation, currents were elicited by a train of 25 depolarizing voltage steps of 200 milliseconds to +60 mV once every 400 milliseconds.

This study was supported by the Ministerio de Ciencia e Innovación (MICINN), Spain (BFU2005-00695, BFU2008-00431 and CSD2008-00005 to A.F. and SAF2006-13893-C02-02 to J.M.F.-F.). L.S. holds fellowships from the MICINN and ‘Fundación La Caixa’. The FI program of the Generalitat de Catalunya supported M.R.-F. and M.P.-V. We thank American Journal Experts for editorial assistance.

References

- Abbott, G. W. and Goldstein, S. A. (2001). Potassium channel subunits encoded by the KCNE gene family: physiology and pathophysiology of the MinK-related peptides (MiRPs). *Mol. Interv.* **1**, 95–107.
- Abbott, G. W. and Goldstein, S. A. (2002). Disease-associated mutations in KCNE potassium channel subunits (MiRPs) reveal promiscuous disruption of multiple currents and conservation of mechanism. *FASEB J.* **16**, 390–400.
- Abbott, G. W., Sesti, F., Splawski, I., Buck, M. E., Lehmann, M. H., Timothy, K. W., Keating, M. T. and Goldstein, S. A. (1999). MiRP1 forms IKr potassium channels with HERG and is associated with cardiac arrhythmia. *Cell* **97**, 175–187.
- Abbott, G. W., Butler, M. H., Bendahhou, S., Dalakas, M. C., Ptacek, L. J. and Goldstein, S. A. (2001). MiRP2 forms potassium channels in skeletal muscle with Kv3.4 and is associated with periodic paralysis. *Cell* **104**, 217–231.
- Attali, B., Romey, G., Honore, E., Schmid-Alliana, A., Mattei, M. G., Lesage, F., Ricard, P., Barhanin, J. and Lazdunski, M. (1992). Cloning, functional expression, and regulation of two K⁺ channels in human T lymphocytes. *J. Biol. Chem.* **267**, 8650–8657.
- Barhanin, J., Lesage, F., Guillemare, E., Fink, M., Lazdunski, M. and Romey, G. (1996). Kv(L)QT1 and IsK (minK) proteins associate to form the I(Ks) cardiac potassium current. *Nature* **384**, 78–80.
- Beeton, C. and Chandy, K. G. (2005). Potassium channels, memory T cells, and multiple sclerosis. *Neuroscientist* **11**, 550–562.
- Beeton, C., Pennington, M. W., Wulff, H., Singh, S., Nugent, D., Crossley, G., Khaytin, I., Calabresi, P. A., Chen, C. Y., Gutman, G. A. et al. (2005). Targeting effector memory T cells with a selective peptide inhibitor of Kv1.3 channels for therapy of autoimmune diseases. *Mol. Pharmacol.* **67**, 1369–1381.
- Beeton, C., Wulff, H., Standifer, N. E., Azam, P., Mullen, K. M., Pennington, M. W., Kolski-Andreaco, A., Wei, E., Grino, A., Counts, D. R. et al. (2006). Kv1.3 channels are a therapeutic target for T cell-mediated autoimmune diseases. *Proc. Natl. Acad. Sci. USA* **103**, 17414–17419.
- Cahalan, M. D., Wulff, H. and Chandy, K. G. (2001). Molecular properties and physiological roles of ion channels in the immune system. *J. Clin. Immunol.* **21**, 235–252.
- Chandrasekhar, K. D., Bas, T. and Kobertz, W. R. (2006). KCNE1 subunits require co-assembly with K⁺ channels for efficient trafficking and cell surface expression. *J. Biol. Chem.* **281**, 40015–40023.
- Chandy, K. G., Wulff, H., Beeton, C., Pennington, M., Gutman, G. A. and Cahalan, M. D. (2004). K⁺ channels as targets for specific immunomodulation. *Trends Pharmacol. Sci.* **25**, 280–289.
- Deschenes, I. and Tomaselli, G. F. (2002). Modulation of Kv4.3 current by accessory subunits. *FEBS Lett.* **528**, 183–188.
- Detre, C., Kiss, E., Varga, Z., Ludanyi, K., Paszty, K., Enyedi, A., Kovacs, D., Panyi, G., Rajnavolgyi, E. and Matko, J. (2006). Death or survival: membrane ceramide controls the fate and activation of antigen-specific T-cells depending on signal strength and duration. *Cell Signal.* **18**, 294–306.
- Folco, E. J., Liu, G. X. and Koren, G. (2004). Caveolin-3 and SAP97 form a scaffolding protein complex that regulates the voltage-gated potassium channel Kv1.5. *Am. J. Physiol. Heart Circ. Physiol.* **287**, H681–H690.
- Freedman, B. D., Fleischmann, B. K., Punt, J. A., Gaulton, G., Hashimoto, Y. and Kotlikoff, M. I. (1995). Identification of Kv1.1 expression by murine CD4-CD8-thymocytes: a role for voltage-dependent K⁺ channels in murine thymocyte development. *J. Biol. Chem.* **270**, 22406–22411.
- Grissmer, S., Dethlefs, B., Wasmuth, J. J., Goldin, A. L., Gutman, G. A., Cahalan, M. D. and Chandy, K. G. (1990). Expression and chromosomal localization of a lymphocyte K⁺ channel gene. *Proc. Natl. Acad. Sci. USA* **87**, 9411–9415.
- Grissmer, S., Ghansani, S., Dethlefs, B., McPherson, J. D., Wasmuth, J. J., Gutman, G. A., Cahalan, M. D. and Chandy, K. G. (1992). The Shaw-related potassium channel gene, Kv3.1, on human chromosome 11, encodes the type I K⁺ channel in T cells. *J. Biol. Chem.* **267**, 20971–20979.
- Grissmer, S., Nguyen, A. N., Aiyar, J., Hanson, D. C., Mather, R. J., Gutman, G. A., Karmilowicz, M. J., Auperin, D. D. and Chandy, K. G. (1994). Pharmacological characterization of five cloned voltage-gated K⁺ channels, types Kv1.1, 1.2, 1.3, 1.5, and 3.1, stably expressed in mammalian cell lines. *Mol. Pharmacol.* **45**, 1227–1234.
- Grunnet, M., Jespersen, T., Rasmussen, H. B., Ljungstrom, T., Jorgensen, N. K., Olesen, S. P. and Klaerke, D. A. (2002). KCNE4 is an inhibitory subunit to the KCNQ1 channel. *J. Physiol.* **542**, 119–130.
- Grunnet, M., Rasmussen, H. B., Hay-Schmidt, A., Rosenstjerne, M., Klaerke, D. A., Olesen, S. P. and Jespersen, T. (2003). KCNE4 is an inhibitory subunit to Kv1.1 and Kv1.3 potassium channels. *Biophys. J.* **85**, 1525–1537.
- Hille, B. (2001). *Ion Channels of Excitable Membranes*. Sunderland, MA: Sinauer.
- Jiang, M., Xu, X., Wang, Y., Toyoda, F., Liu, X. S., Zhang, M., Robinson, R. B. and Tseng, G. N. (2009). Dynamic partnership between KCNQ1 and KCNE1 and influence on cardiac IKS current amplitude by KCNE2. *J. Biol. Chem.* **284**, 16452–16462.
- Jou, I., Pyo, H., Chung, S., Jung, S. Y., Gwag, B. J. and Joe, E. H. (1998). Expression of Kv1.5 K⁺ channels in activated microglia in vivo. *Glia* **24**, 408–414.
- Krumer, M., Gao, X., Bian, J. S., Melman, Y. F., Kagan, A. and McDonald, T. V. (2004). An LQT mutant minK alters KvLQT1 trafficking. *Am. J. Physiol. Cell Physiol.* **286**, C1453–C1463.
- Levy, D. I., Wanderling, S., Biemesderfer, D. and Goldstein, S. A. (2008). MiRP3 acts as an accessory subunit with the BK potassium channel. *Am. J. Physiol. Renal Physiol.* **295**, F380–F387.
- Lewis, A., McCrossan, Z. A. and Abbott, G. W. (2004). MinK, MiRP1, and MiRP2 diversify Kv3.1 and Kv3.2 potassium channel gating. *J. Biol. Chem.* **279**, 7884–7892.
- Lewis, R. S. and Cahalan, M. D. (1995). Potassium and calcium channels in lymphocytes. *Annu. Rev. Immunol.* **13**, 623–653.
- Li, Y., Um, S. Y. and McDonald, T. V. (2006). Voltage-gated potassium channels: regulation by accessory subunits. *Neuroscientist* **12**, 199–210.
- Liu, Q. H., Fleischmann, B. K., Hondowicz, B., Maier, C. C., Turka, L. A., Yui, K., Kotlikoff, M. I., Wells, A. D. and Freedman, B. D. (2002). Modulation of Kv channel expression and function by TCR and costimulatory signals during peripheral CD4(+) lymphocyte differentiation. *J. Exp. Med.* **196**, 897–909.
- Lundquist, A. L., Turner, C. L., Ballester, L. Y. and George, A. L., Jr (2006). Expression and transcriptional control of human KCNE genes. *Genomics* **87**, 119–128.
- Maguy, A., Hebert, T. E. and Nattel, S. (2006). Involvement of lipid rafts and caveolae in cardiac ion channel function. *Cardiovasc. Res.* **69**, 798–807.
- Manganas, L. N. and Trimmer, J. S. (2000). Subunit composition determines Kv1 potassium channel surface expression. *J. Biol. Chem.* **275**, 29685–29693.
- Martens, J. R., Kwak, Y. G. and Tamkun, M. M. (1999). Modulation of Kv channel alpha/beta subunit interactions. *Trends Cardiovasc. Med.* **9**, 253–258.
- Martens, J. R., Navarro-Polanco, R., Coppock, E. A., Nishiyama, A., Parshley, L., Grobaski, T. D. and Tamkun, M. M. (2000). Differential targeting of Shaker-like potassium channels to lipid rafts. *J. Biol. Chem.* **275**, 7443–7446.
- Martens, J. R., O’Connell, K. and Tamkun, M. (2004). Targeting of ion channels to membrane microdomains: localization of KV channels to lipid rafts. *Trends Pharmacol. Sci.* **25**, 16–21.
- Martinez-Marmol, R., Villalonga, N., Sole, L., Vicente, R., Tamkun, M. M., Soler, C. and Felipe, A. (2008). Multiple Kv1.5 targeting to membrane surface microdomains. *J. Cell Physiol.* **217**, 667–673.
- McCormack, T., McCormack, K., Nadal, M. S., Vieira, E., Ozaita, A. and Rudy, B. (1999). The effects of Shaker beta-subunits on the human lymphocyte K⁺ channel Kv1.3. *J. Biol. Chem.* **274**, 20123–20126.
- McCrossan, Z. A. and Abbott, G. W. (2004). The MinK-related peptides. *Neuropharmacology* **47**, 787–821.
- McCrossan, Z. A., Lewis, A., Panaghie, G., Jordan, P. N., Christini, D. J., Lerner, D. J. and Abbott, G. W. (2003). MinK-related peptide 2 modulates Kv2.1 and Kv3.1 potassium channels in mammalian brain. *J. Neurosci.* **23**, 8077–8091.
- McCrossan, Z. A., Roepke, T. K., Lewis, A., Panaghie, G. and Abbott, G. W. (2009). Regulation of the Kv2.1 potassium channel by MinK and MiRP1. *J. Membr. Biol.* **228**, 1–14.
- Melman, Y. F., Um, S. Y., Krumer, M., Kagan, A. and McDonald, T. V. (2004). KCNE1 binds to the KCNQ1 pore to regulate potassium channel activity. *Neuron* **42**, 927–937.
- Michelsen, K., Yuan, H. and Schwappach, B. (2005). Hide and run. Arginine-based endoplasmic-reticulum-sorting motifs in the assembly of heteromultimeric membrane proteins. *EMBO Rep.* **6**, 717–722.
- Mullen, K. M., Rozycka, M., Rus, H., Hu, L., Cudrici, C., Zafrańska, E., Pennington, M. W., Johns, D. C., Judge, S. I. and Calabresi, P. A. (2006). Potassium channels Kv1.3 and Kv1.5 are expressed on blood-derived dendritic cells in the central nervous system. *Ann. Neurol.* **60**, 118–127.
- Nagaya, N. and Papazian, D. M. (1997). Potassium channel alpha and beta subunits assemble in the endoplasmic reticulum. *J. Biol. Chem.* **272**, 3022–3027.
- Panyi, G., Varga, Z. and Gaspar, R. (2004a). Ion channels and lymphocyte activation. *Immunol. Lett.* **92**, 55–66.
- Panyi, G., Vamosi, G., Bacsó, Z., Bagdany, M., Bodnar, A., Varga, Z., Gaspar, R., Matyus, L. and Damjanovich, S. (2004b). Kv1.3 potassium channels are localized in the immunological synapse formed between cytotoxic and target cells. *Proc. Natl. Acad. Sci. USA* **101**, 1285–1290.
- Rocheleau, J. M., Gage, S. D. and Kobertz, W. R. (2006). Secondary structure of a KCNE cytoplasmic domain. *J. Gen. Physiol.* **128**, 721–729.

- Roepke, T. K., Kontogeorgis, A., Ovanez, C., Xu, X., Young, J. B., Purtell, K., Goldstein, P. A., Christini, D. J., Peters, N. S., Akar, F. G. et al. (2008). Targeted deletion of *kcnk2* impairs ventricular repolarization via disruption of I(K_{slow}) and I(to,f). *FASEB J.* **22**, 3648-3660.
- Sharma, N., Crane, A., Clement, J. P. t., Gonzalez, G., Babenko, A. P., Bryan, J. and Aguilar-Bryan, L. (1999). The C terminus of SUR1 is required for trafficking of KATP channels. *J. Biol. Chem.* **274**, 20628-20632.
- Szabo, I., Adams, C. and Gulbins, E. (2004). Ion channels and membrane rafts in apoptosis. *Pflugers Arch.* **448**, 304-312.
- Szabo, I., Bock, J., Grassme, H., Soddemann, M., Wilker, B., Lang, F., Zoratti, M. and Gulbins, E. (2008). Mitochondrial potassium channel Kv1.3 mediates Bax-induced apoptosis in lymphocytes. *Proc. Natl. Acad. Sci. USA* **105**, 14861-14866.
- Um, S. Y. and McDonald, T. V. (2007). Differential association between HERG and KCNE1 or KCNE2. *PLoS ONE* **2**, e933.
- Vicente, R., Escalada, A., Coma, M., Fuster, G., Sanchez-Tillo, E., Lopez-Iglesias, C., Soler, C., Solsona, C., Celada, A. and Felipe, A. (2003). Differential voltage-dependent K⁺ channel responses during proliferation and activation in macrophages. *J. Biol. Chem.* **278**, 46307-46320.
- Vicente, R., Escalada, A., Soler, C., Grande, M., Celada, A., Tamkun, M. M., Solsona, C. and Felipe, A. (2005). Pattern of Kv beta subunit expression in macrophages depends upon proliferation and the mode of activation. *J. Immunol.* **174**, 4736-4744.
- Vicente, R., Escalada, A., Villalonga, N., Texido, L., Roura-Ferrer, M., Martin-Satue, M., Lopez-Iglesias, C., Soler, C., Solsona, C., Tamkun, M. M. et al. (2006). Association of Kv1.5 and Kv1.3 contributes to the major voltage-dependent K⁺ channel in macrophages. *J. Biol. Chem.* **281**, 37675-37685.
- Vicente, R., Villalonga, N., Calvo, M., Escalada, A., Solsona, C., Soler, C., Tamkun, M. M. and Felipe, A. (2008). Kv1.5 association modifies Kv1.3 traffic and membrane localization. *J. Biol. Chem.* **283**, 8756-8764.
- Villalonga, N., Escalada, A., Vicente, R., Sanchez-Tillo, E., Celada, A., Solsona, C. and Felipe, A. (2007). Kv1.3/Kv1.5 heteromeric channels compromise pharmacological responses in macrophages. *Biochem. Biophys. Res. Commun.* **352**, 913-918.
- Wulff, H. and Pennington, M. (2007). Targeting effector memory T-cells with Kv1.3 blockers. *Curr. Opin. Drug Discov. Devel.* **10**, 438-445.
- Wulff, H., Beeton, C. and Chandy, K. G. (2003). Potassium channels as therapeutic targets for autoimmune disorders. *Curr. Opin. Drug Discov. Devel.* **6**, 640-647.
- Zuzarte, M., Heusser, K., Renigunta, V., Schlichthorl, G., Rinne, S., Wischmeyer, E., Daut, J., Schwappach, B. and Preisig-Muller, R. (2009). Intracellular traffic of the K⁺ channels TASK-1 and TASK-3: role of N- and C-terminal sorting signals and interaction with 14-3-3 proteins. *J. Physiol.* **587**, 929-952.